P6.10 A NUMERICAL STUDY ON CHARACTERISTICS OF INTERNAL GRAVITY WAVES IN THE STRATOSPHERE INDUCED BY MESOSCALE CONVECTIVE SYSTEM

Song, In-Sun, and Hye-Yeong Chun*
Department of Atmospheric Sciences, Yonsei University, Seoul, Korea

1. INTRODUCTION

It is well known that the vertically propagating internal gravity waves can have profound effects on the large-scale circulation in the middle atmosphere. Fritts (1984) observed that high-frequency gravity waves are ubiquitous in the middle atmosphere. Bergman and Salby (1994) showed the upward propagation of energy and momentum of high frequency waves is dominant in the tropical stratosphere. Thus cumulus convection can be considered as a major gravity wave source in the tropical region and the storm track region of the Northern Hemisphere. Chun and Baik (1998) theoretically investigated the thermally induced internal gravity waves. They showed that the wave breaking above the cloud top can change basic-state wind by 6 m s^{-1} / day. This amount of the wave drag is comparable to that calculated using the parameterization of the orographically generated gravity waves. Recently, Chun et al. (2001) investigated the effects of GWDC on the large-scale circulation using a general circulation model in which the GWDC parameterization developed by Chun and Baik is implemented.

Importance of convection as a source of gravity waves has become recognized, and there have been several attempts to examine the mechanisms of the convetively generated gravity waves. There are two proposed mechanisms for internal gravity waves induced by convective clouds. Clark et al. (1986) proposed obstacle or thermal forcing mechanism that convective cloud acts like an obstacle to the flow and gravity waves can be generated when the basic-state wind relative to the convective cell is not zero. Analytical studies of the response of the stable atmosphere to a specified thermal forcing (e.g., Lin and Smith 1986; Nicholls et al. 1991; Chun and Lin 1995) can be categorized in this thermal forcing mechanism. Their results could account for some basic features of gravity waves simulated by sophisticated numerical models. Fovell et al. (1992) proposed the mechanical oscillator mechanism that strong updrafts in convective system can stimulate the statically stable stratosphere and thus generate internal gravity waves in the stratosphere under a zero storm-relative basic-state wind condition. Alexander et al. (1995) also accounted for characteristics of convectively generated gravity waves using this mechanism.

In this study, we investigate characteristics of convectively generated internal gravity waves using two-dimensional cloud-resolving model by comparing the mechanical oscillator mechanism with thermal forcing mechanism

*Corresponding author address: Prof. Hye-Yeong Chun, Department of Atmospheric Sciences, Yonsei University, Shinchon-dong, Seodaemun-ku, Seoul 120-749, Korea.
E-mail : chy@atmos.yonsei.ac.kr

2. NUMERICAL SIMULATION

2.1 Numerical model

In this study, mesoscale convective systems are simulated using ARPS (Advanced Regional Prediction System) (Xue et al. 1995) model developed in CAPS (Center for Analysis and Prediction of Storms) of University of Oklahoma. ARPS is a 3-dimensional, nonhydrostatic, and compressible model calculating mixing ratios of cloud, rain, and ice phases explicitly. In this study, 2-dimensional (x-z) version of ARPS with Kessler type warm rain microphysics is used. Smagorinsky's 1st order closure is used for subgrid scale turbulence parameterization. The model domain is 1200 km wide and 50 km depth. Horizontal and vertical grid intervals are 1 km and 300 m, respectively. At upper boundary, a sponge layer of 15 km depth is included, and Klemp, Lilly, Durran radiation condition based on Orlanski (1976) radiation condition is employed at the lateral boundaries. In time integration, big time step (Δt) and small time step (δt) are 3 s and 1 s, respectively.

The analytic sounding of Weisman and Klemp (1982) is used as the basic-state thermodynamic structure for all simulations in this study. Bouyancy frequencies calculated from the basic state thermodynamic structure are about 0.01 s^{-1} and 0.022 s^{-1} in the troposphere and stratosphere, respectively. Basic-state wind has a linear shear layer below z = 6 km and a constant value above.

2.2 Simulation results

Three numerical simulations were performed to investigate the mechanisms of convectively generated internal gravity waves. The control case (CTR) was simulated for 12 hr. The convection in the CTR was initiated by an ellipsoidal bubble with the maximum potential temperature perturbation of 2 K located in x = 800 km and z = 1.5 km. The convective storm in the CTR reaches a quasi-steady state after t = 4 hr. Convective cells are regularly regenerated from the quasi-steady gust front and propagated rearward relative to the gust front. Figure 1 shows the vertical velocity contours of w = 2 m s^{-1} superimposed on total potential temperature field in the CTR at t = 3 hr and t = 5 hr. At t = 3 hr, the convective cells are upright and the horizontal propagation of gravity waves in the stratospehre is almost isotropic. Contrary, at t = 5 hr, the convective cells are tilted rearward, and the gravity waves mainly propagate to the west.

To compare the differences between the thermal forc-

ing mechanism and the mechanical oscillator mechanism, two dry simulations were performed. The one (DRYM) is forced by vertical momentum, and the other (DRYH) is forced by diabatic heating and cooling. In order to obtain such forcings used in the DRYM and DRYH, the vertical velocity and diabatic forcing fields were saved at 1-min interval from t = 4 hr to 12 hr in the CTR.

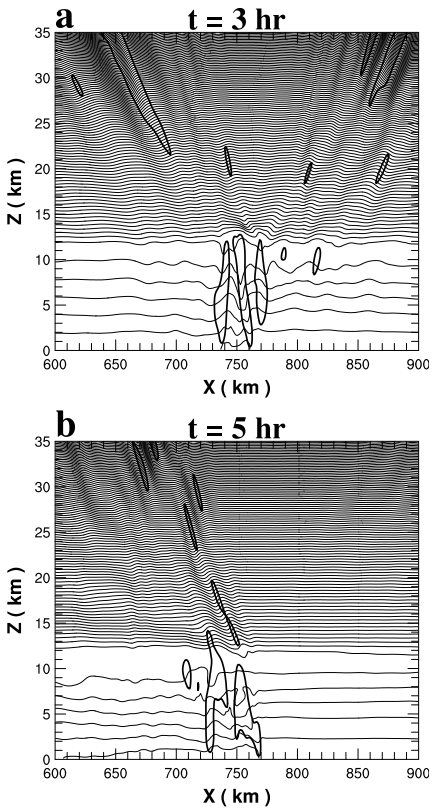

Figure 1. The vertical velocity contours of w = 2 m s^{-1} superimposed on total potential temperature field in the CTR at (a) t = 3 hr and (b) t = 5 hr . The contour interval for total potential temperature is 7 K. The vertical velocity contours are plotted with thick lines.

In the DRYM, the vertical velocities larger than 2.8 m s^{-1} in the CTR were used as the vertical momentum forcing to represent updraft of individual convective cell. The vertical velocity is gradually adjusted to the vertical momentum forcing (w_{ctr}) for 1-min period:

$$\frac{\partial \overline{\rho} w}{\partial t} + \cdots = \overline{\rho}\left(\frac{2 \times w_{ctr}}{60 sec} - \gamma w\right) , \qquad (1)$$

where γ is the coefficient to adjust the vertical velocity (w) simulated in the DRYM to the given vertical momentum forcing:

$$\gamma = \begin{cases} 1/120.\ \mathrm{s}^{-1} & w_{ctr} = 0.0 , \\ 1/480.\ \mathrm{s}^{-1} & w_{ctr} \neq 0.0 , \end{cases} \qquad (2)$$

where γ = 0.0 above z = 15 km.

In the DRYH, the adjustment process in the DRYM is not needed because heating and cooling rate fields can be directly obtained from the CTR. In order to make the spatial scale of the diabatic forcing similar to that of vertical momentum forcing, the portion of the diabatic forcing field where the magnitude of heating and cooling exceeds 0.004 K s^{-1} was used.

Figure 2 shows the total potential temperature fields in the CTR, DRYM, and DRYH. The field variables in the CTR at t = 8 hr are equivalent to those in the DRYM and DRYH at t = 4 hr because the DRYM and DRYH are simulated using forcings obtained during the period from t = 4 hr to 12 hr in the CTR. In Fig. 2c, the magnitude of potential temperature perturbation is two times reduced for the convenience of comparison with the CTR and DRYM. In all three simulations, active gravity wave fields are simulated in the stratosphere above the convectively active region in the troposphere. The phase lines in the active gravity wave fields are slightly tilted to the vertical. Such a phase line structure means that the gravity waves above the convectively active region are high-frequency waves as indicated by Fovell et al. (1992). The gravity waves with the phase lines largely tilted to the vertical exist in the rear side of convective storms in the CTR and DRYH. In the DRYM, however, the gravity waves with largely tilted phase lines to the vertical are weak relative to the CTR and DRYH.

3. SPECTRAL ANALYSIS

To examine the differences in the characteristics of the stratospheric gravity waves produced in the three simulations, power spectral densities (PSDs) of vertical velocity field as a function of vertical and horizontal wavelengths and period were calculated. For the spectral analysis, vertical velocity fields from t = 6 hr to 12 hr were used in the CTR, and those from t = 2 hr to 8 hr were used in the DRYM and DRYH. The PSDs were calculated separately for the eastward and westward propagating waves in the stratosphere because the horizontal propagation of the waves in the stratosphere is anisotropic in the quasi-steady state. The region used for the spectral analysis is 900 km (x = 170 – 1070 km) wide and 20 km depth above z = 15 km for all simulations.

From the PSDs, it is found that the dominant vertical wavelengths range from 6.8 km to 10 km in all simulations. The spectral peak is located at λ_z = 6.8 km for the CTR and DRYM and λ_z = 10 km for the DRYH. The similarity of the dominant vertical wavelength range in the DRYM and DRYH is because the vertical scale of vertical momentum forcing is almost the same as that of diabatic forcing. The westward propagating gravity waves simulated in the CTR and DRYH have the dominant horizontal wavelength range of 10 – 200 km. However, the waves possessing the horizontal wavelengths exceeding 30 km are very weak in the DRYM. Although the wave forcings used in the DRYM and DRYH are confined in the convectively active region in the CTR and the horizontal scales of the individual diabatic heating and vertical momentum

forcing are similar, the waves with large horizontal wavelength can be better simulated in the DRYH than in the DRYM.

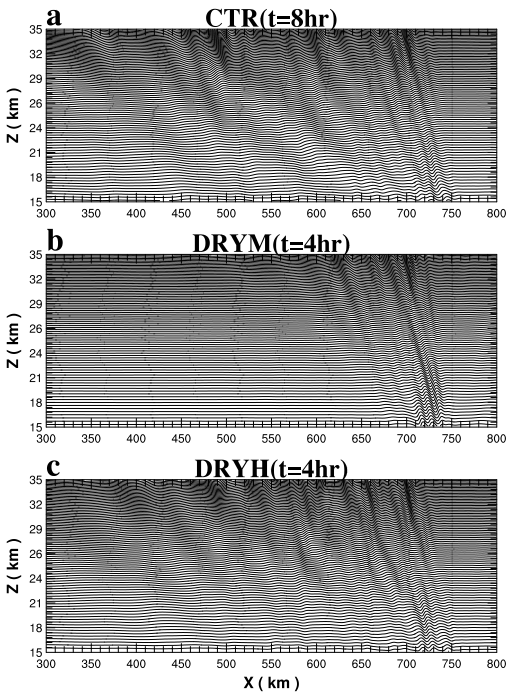

Figure 2. Total potential temperature field in the (a) CTR, (b) DRYM, and (c) DRYH. Contour interval for total potential temperature is 7 K. Note that the magnitude of potential temperature perturbations in Fig. 2c is two times reduced for the convenience of comparison with the CTR and DRYM.

The westward propagating gravity waves have the dominant periods of 10 – 70 min in the CTR and DRYH. However, the waves in the DRYM have the dominant periods of 10 – 20 min. In the DRYM and DRYH, temporal characteristics of the specified wave forcings are almost the same. Nevertheless, gravity waves in the stratosphere simulated in the DRYM do not represent well the low frequency part in the spectrum.

Figure 3 shows the PSDs as a function of storm relative phase speed. For all three simulations, the storm relative phase speeds of the westward propagating gravity waves in the stratosphere range from - 60 m s^{-1} to - 6 m s^{-1}, and the dominant peaks are located in the phase speeds of - 25 m s^{-1} – -18 m s^{-1}. In Fig. 3, it is notable that the gravity waves with phase speeds less than - 40 m s^{-1} are very weak in the DRYM. Through the spectral analysis, it is found that the gravity wave modes with large horizontal wavelength, low frequency, and phase speeds less than - 40 m s^{-1} are much weaker in the DRYM than those in the CTR and DRYH.

In order to understand the differences in the gravity wave characteristics analyzed in the DRYM and DRYH, the horizontal wavelength PSDs of vertical velocity and diabatic forcings in the CTR were calculated (Fig. 4). The

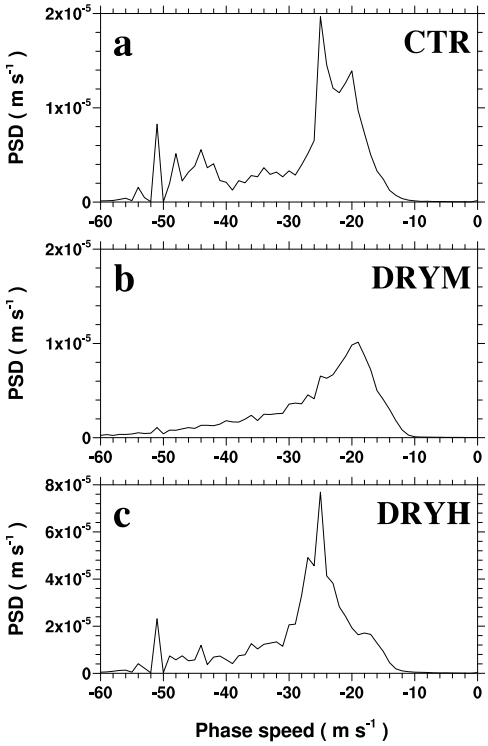

Figure 3. Power spectral densities of westward propagating gravity waves in the stratosphere as a function of horizontal phase speed relative to the storm propagation in the (a) CTR, (b) DRYM, and (c) DRYH.

PSD of the diabatic forcing have two peaks with similar magnitude at λ_x = 12.5 km and 46.23 km, while the PSD of the vertical velocity forcing has a one peak near λ_x = 12.5 km and the spectral power of the vertical velocity forcing monotonically decreases with the horizontal wavelength. The PSD of the diabatic forcing can be represented as the sum of the PSDs of the diabatic heating and cooling and the cospectra of the heating and cooling. In both the PSDs of the diabatic heating and cooling, there exists a spectral peak at λ_x = 46.23 km. From the cospectra, it is also found that the spectral power of diabatic forcing at λ_x = 46.23 km becomes larger than that of diabatic heating due to the effect of the diabatic cooling (not shown).

4. SUMMARY

In this study, the mechanisms for internal gravity waves in the stratosphere induced by convective storms simulated by two-dimensional cloud model are investigated through the spectral analysis of the gravity waves and wave forcing fields. In the CTR, mesoscale convective system is simulated using cloud microphysics. In the DRYM and DRYH, the dry simulations forced by the vertical momentum forcng and diabatic forcing are performed, respectively. These forcings are obtained from the CTR saved for every 1 min.

In the spectral analysis of the gravity waves in the

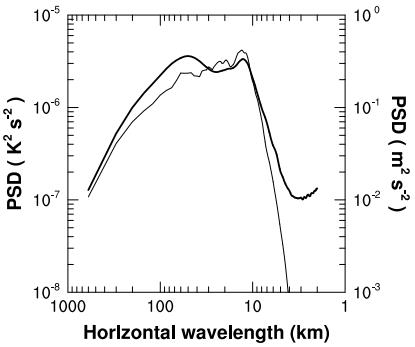

Figure 4. Power spectral density (PSD) of diabatic forcing (thick solid) and vertical velocity forcing (solid) in the CTR as a function of horizontal wavelength.

stratosphere, the dominant vertical wavelengths are not significantly different for all simulations because the vertical scales of individual vertical momentum forcing and diabatic forcing are almost identical. However, in the DRYM, the gravity waves with large horizontal wavelengths, low frequency, and the phase speeds less than - 40 m s^{-1} are very weak compared with the DRYH. These differences of the characteristics of gravity waves in the DRYM and DRYH are due to the fact that the dominant horizontal scale of the diabatic forcing is larger than that of the vertical momentum forcing. The diabatic forcing has two spectral peaks at λ_x = 12.5 and 46.23 km, while the vertical momentum forcing has a spectral peak at λ_x = 12.5 km. It is found that the PSD of diabatic forcing becomes dominant at λ_x = 46.23 due to the effect of diabatic cooling as well as the diabatic heating.

5. ACKNOWLEDGEMENT

This research was supported by the Climate Environment System Research Center sponsored by the SRC program of Korea Science and Engineering Foundation and Brain Korea 21 program.

6. REFERENCES

Alexander, M. J., J. R. Holton, and D. R. Durran, 1995: The gravity wave response above deep convection in a squall line simulation. *J. Atmos. Sci.,* **52,** 2212–2226.

Bergman, J. W., and M. L. Salby, 1994: Equatorial wave activity generated by fluctuations in observed convection. *J. Atmos. Sci.,* **51,** 3791–3806.

Chun, H.-Y., and Y.-L. Lin, 1995: Enhanced response of an atmospheric flow to a line-type heat sink in the presence of a critical level. *Meteor. Atmos. Phys.,* **55,** 33–45.

____, and J.-J. Baik, 1998: Momentum flux by thermally induced internal gravity waves and its approximation for large-scale models. *J. Atmos. Sci.,* **55,** 3299–3310.

____, M.-D. Song, J.-W. Kim, and J.-J. Baik, 2001: Effects of gravity wave drag induced by cumulus convection on atmospheric general circulation. *J. Atmos. Sci.,* **58,** 302–319.

Clark, T. L., T. Hauf, and J. P. Kuettner, 1986: Convectively forced internal gravity waves: Results from two-dimensional numerical experiments. *Quart. J. Roy. Meteor. Soc.,* **112,** 899–925.

Fovell, R. G., D. Durran, and J. R. Holton, 1992: Numerical simulations of convectively generated stratosphere gravity waves. *J. Atmos. Sci.,* **49,** 1427–1442.

Fritts, D. C., 1984: Gravity wave saturation in the middle atmosphere: A review of theory and observations. *Rev. Geophys. Space Phys.,* **22,** 275–308.

Lin, Y. L., and R. B. Smith, 1986: Transient dynamics of airflow near a local heat source. *J. Atmos. Sci.,* **43,** 40–49.

____, and H.-Y. Chun, 1991: Effects of diabatic cooling in a shear flow with a critical level. *J. Atmos. Sci.,* **48,** 2476–2491.

Nicholls, M. E., R. A. Pielke, and W. R. Cotton, 1991: Thermally forced gravity waves in an atmosphere at rest. *J. Atmos. Sci.,* **48,** 1869–1884.

Orlanski, I., 1976: A simple boundary condition for unbounded hyperbolic flows. *J. Comput. Phys.,* **21,** 251–269.

Weisman, M. L., and J. B. Klemp, 1982: The dependence of numerically simulated convective storms on wind shear and buoyancy. *Mon. Wea. Rev.,* **110,** 504–529.

Xue, M., K. K. Droegemeier, V. Wong, A. Shapiro, and K. Brewster, 1995: *ARPS version 4.0 User's Guide.* Center for Analysis and Prediction of Storms, University of Oklahoma, 380pp.